# Pseudorotational Intersystem Crossing in $d^6$ Complexes

**Keith F. Purcell**

*Contribution from the Department of Chemistry, Kansas State University, Manhattan, Kansas 66506.* *Received January 16, 1979*

**Abstract:** Intersystem crossings along the trigonal and rhombic twisting coordinates for a low-spin, six-coordinate, $d^6$ complex (e.g., $Fephen_3^{2+}$) are examined computationally. Molecular terms, including configuration interaction and spin–orbit coupling, are developed within the context of the angular overlap model. The Landau-Zener treatment of intersystem crossing yields a rate constant for racemization compatible with that of experiment and lends support to the interpretations of kinetic data that intersystem crossing is an integral part of the racemization process for $Fephen_3^{2+}$. A brief examination of photoinduced racemization is given and implications for spin-equilibria complexes are discussed.

## Introduction

Recently we reported[1] on solution NMR studies of a complex from the class $Fephen_2X_2$, in which X = $NCBPh_3^-$ and phen = 1,10-phenanthroline. This complex was characterized as having a spin-singlet ground state in the solid at room temperature and in $CH_2Cl_2$ solution at 221 K. On warming, this complex exhibits synchronous enantiomerization and spin-state isomerization ($S = 0 \rightleftarrows S = 2$). At 275 K, the intramolecular racemization rate constant is greater than $10^2$ $s^{-1}$, at least six powers of ten greater than the rate constant[2] at 300 K for the unimolecular chirality change of $Fephen_3^{2+}$.

These results suggest a strong link between the rate of racemization and intersystem crossing efficiency, an idea which seems to have first occurred to Davies in 1954.[3] To explore this possibility we have written programs to calculate the singlet, triplet, and quintet molecular term energies for $d^6$ complexes, including configuration interaction and spin–orbit coupling. The basic question which we hoped to answer is: does intersystem crossing arise along an intramolecular twisting coordinate and, if so, at an energy and frequency compatible with the racemization rates for $Fephen_3^{2+}$ and $Fephen_2(NCBPh_3)_2$? Here we will focus only on the metal ion electronic energy influence on the barrier to a chirality change.

## Methods

The angular overlap model[4] (AOM) is used to construct bases of d-type MOs at each point along a selected reaction coordinate. Slater determinants are constructed in these bases and those linear combinations of determinants which are diagonal under $\hat{S}^2$ are constructed. These spin-diagonal functions are then used to generate a matrix at each structure for the electron repulsion operator, $e^2/r$. Diagonalization of this matrix yields the term energies and wave functions for each molecular structure. The results are presented graphically as potential energy curves.

One set of computations was performed using the $e_\sigma$ parameter of 0.585 $\mu m^{-1}$ appropriate for $Fe^{2+}$–phen[5] (in the AOM $e_\sigma$ represents the increase in the one-electron energy of the $d_{z^2}$ orbital when overlapped by a lone pair orbital of the ligand). The Racah parameters $B$ and $C$ for d/d electron repulsion were chosen to be 0.073 and 0.292 $\mu m^{-1}$, respectively, in accordance with the studies of König.[6] These parameter choices were intended to be representative, rather than precise, in keeping with the purpose of the study.

Modes for pseudorotation in six-coordinate molecules have been thoroughly analyzed by Musher.[7] The modes designated $M_3'$ and $M_3''$ correspond, for $Fephen_3^{2+}$, to the rigid-ring Bailar twists of Springer and Sievers[8] and of Rây and Dutt,[9] respectively. These are the modes we have chosen to examine here.

The $M_3'$ mode is characterized by the antiprism angle $\Phi$ in Figure 1. The rigid ring constraint ($\alpha = \angle NFeN = 80°$ for phen) serves to specify, for each choice of $\Phi$, the ring cant to the $C_3$ axis (angle $\psi = 35.26°$ for $O_h$) and the $\theta$ coordinate of each nitrogen atom. The symmetry of $Fephen_3^{2+}$ is $D_3$ at all points along the $M_3'$ reaction coordinate, except at the transition state, where new symmetry elements arise[10] and the point group becomes $D_{3h}$.

The $M_3''$ mode, otherwise known as the rhombic twist pathway, can be readily described in terms of the $\theta$ coordinate of the intraligand $C_2$ axis ($C_{2l}$); the ligand rings define mutually orthogonal planes throughout the motion. The $M_3''$ mode breaks down the initial $D_3$ symmetry to $C_2$ along the reaction coordinate, and leads to a $C_{2v}$ transition state structure. This mode is of A symmetry, of course, under the $C_2$ group and leads to more thorough mixing of basis MOs and configurations than does the $M_3'$ mode.

The spin–orbit calculations were performed with $\zeta = 0.042$ $\mu m^{-1}$, again in accordance with König.[6] The molecular term wave functions as linear combinations of Slater determinants from the CI calculations were used as basis functions for setting up the spin–orbit matrix. The latter was diagonalized using the EISPACK system.[11]

## Results

**d Orbital Energies.** The d* MO energies as a function of reaction coordinate are given in Figure 2 (the superscript * is a reminder that the d orbitals of the complex are antibonding in nature). Set (A) corresponds to the $M_3'$ mode while set (B) derives from the $M_3''$ mode. The general lowering in energy of the upper two orbitals and raising of the lower three reflects a transfer of $\sigma^*$ character to the lower set. Several points can be made about these results before proceeding to the CI results.

The structure for $M_3'$ at $\Phi = 30°$ actually corresponds to a trigonally flattened complex ($\Phi = 30°$, $\alpha = 80°$ requires $\Psi > 35.26°$). The energy splitting of the $t^*_{2g}$ MOs by the trigonal symmetry component is clearly evident and initially diminishes as $\Phi$ decreases. The a and e orbitals cross very slightly before the ring cant angle $\Psi$ reaches the $O_h$ value of 35.26°. The diagonal elements of the e block of the ligand field matrix (shown as dashed lines) and the e eigenvalues depend on $\Phi$ in inverted ways, revealing that the angle dependences of the e MO energies are dominated by the ligand field mixing ($\xi \leftrightarrow \epsilon$ and $\eta \leftrightarrow \zeta$, where $\xi \sim d_{yz}$, $\eta \sim d_{xz}$, $\epsilon \sim d_{x^2-y^2}$, $\zeta \sim d_{xy}$, $\Theta \sim d_{z^2}$). The variation in the energy of MO $a_1$ is due solely to the nodal characteristics of $d_{z^2}$ as the ligand lone pairs traverse the conical $d_{z^2}$ nodal surfaces. There are no instances of symmetry-forbidden crossing of basis levels along $M_3'$.

This latter point does not apply to the $M_3''$ mode. The $\Theta$ and $(\xi - \eta)$ basis orbitals have symmetry a under the $C_2$ group and their intended crossing (dashed lines) is *strongly* avoided along

0002-7863/79/1501-5147$01.00/0 

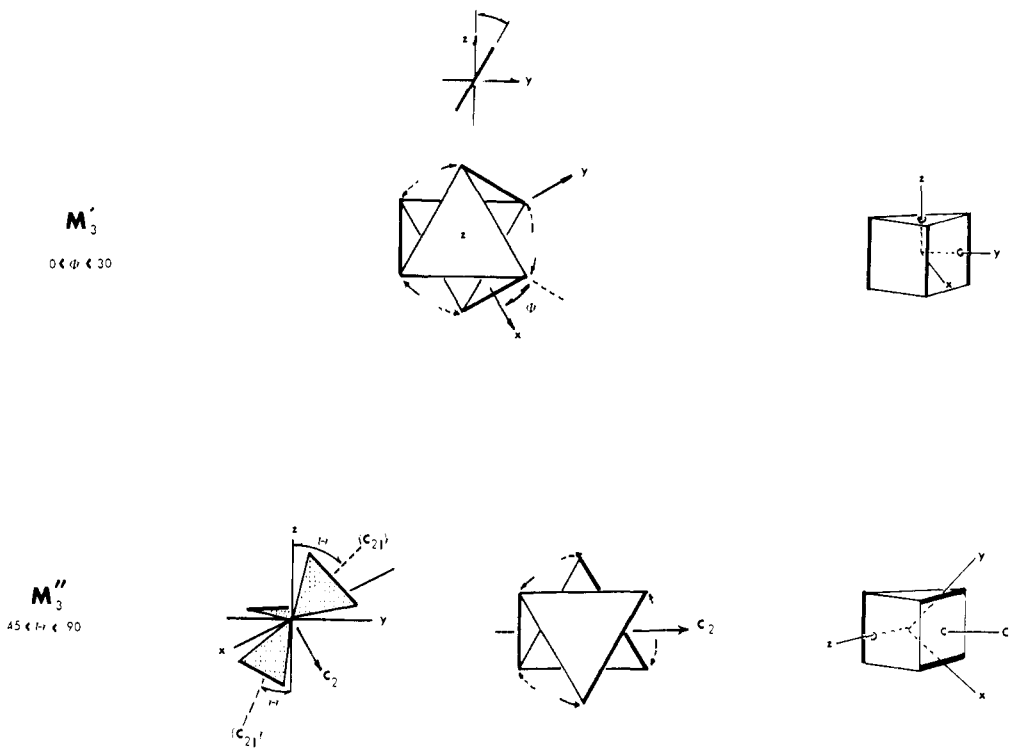


**Figure 1.** The coordinate systems, atom displacement vectors, and transition-state structures for pseudorotation by the trigonal twist ($M_3'$) and rhombic twist ($M_3''$) mechanism for $M(LL)_3$.

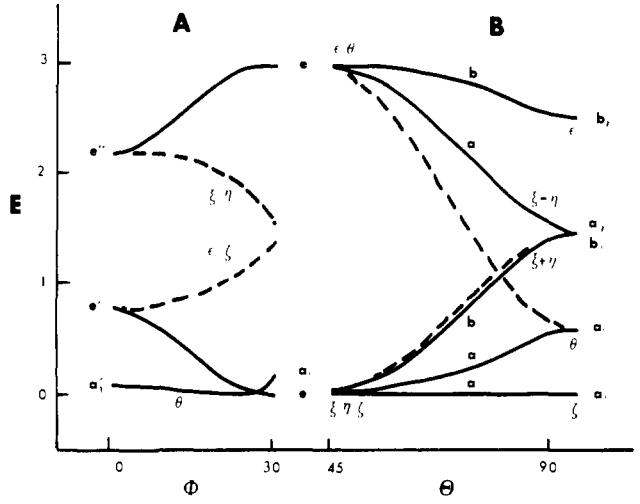


**Figure 2.** AOM orbital energies (in units of $e_\sigma$ = 0.585 $\mu$m) as functions of (A) $\Phi$ and (B) $\Theta$.

the reaction path. The interaction is so strong that no maximum in the energy of $(\xi - \eta) \rightarrow \Theta$ appears at $\Theta \sim 80°$ (were there to be a maximum, a molecule with the lowest singlet configuration could experience a barrier at $\Theta \sim 80°$ with the rhombic prism structure at $\Theta = 90°$ then corresponding to an intermediate). Also to be noted are the weaker (noncrossing) interactions of $\zeta$ with $\Theta$ and $(\xi - \eta)$ and of $\epsilon$ with $(\xi + \eta)$.

A final point regarding Figure 2B is that the $\xi$, $\eta$ MOs are "accidentally" degenerate at the transition state (an example of an allowed "crossing", or more properly "tangency"). This situation places great demands on the CI study because one is forced to consider the entire set of 100 Slater determinants with $M_S = 0$, so as not to violate the degeneracy feature at $\Theta = 90°$.

These diagrams (excluding electron repulsion) suggest that the $(a_1)^2(e)^4$ and $(a)^2(a)^2(b)^2$ configurations favor the $D_3$ structure; the $(a_1)^2(e)^2(e)^2$ configuration weakly (because of the small maximum for $\Theta$ at $\Phi = 0°$) favors the $D_3$ structure, whereas the high-spin configuration should be highly fluxional along the $M_3''$ coordinate, insofar as the d-orbital energies are concerned.

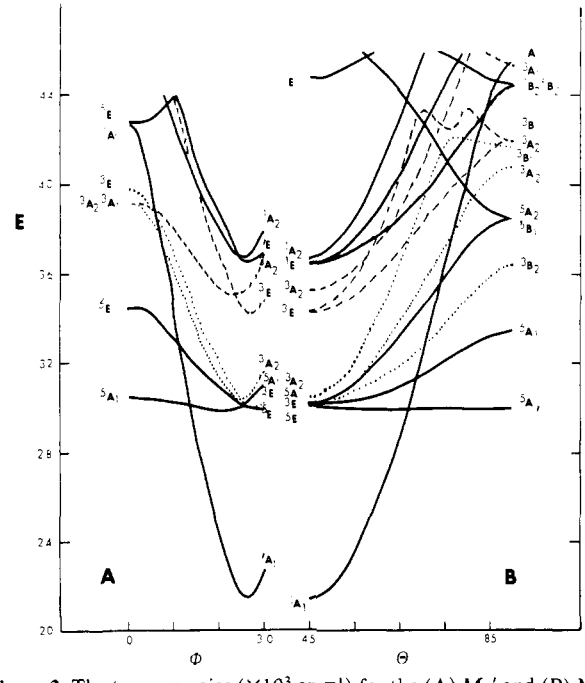


**Figure 3.** The term energies ($\times 10^3$ cm$^{-1}$) for the (A) $M_3'$ and (B) $M_3''$ modes.

**Potential Surface Characteristics.** The term energies derived from Figure 2 are given in Figures 3A for $M_3'$ and 3B for $M_3''$. Only terms derived from the $O_h$ terms $^1A_{1g}$, $^1T_{1g}$, $^1T_{2g}$, $^3T_{1g}$, $^3T_{2g}$, $^5T_{2g}$, and $^5E_g$ have been included, for the sake of simplicity. Several items are of interest in this figure. Configuration interaction is of importance to all terms except those of

**Table I.** Linealogy of Spin-Orbit Terms

| $O_h$ | $C_2$ | $C_2'$ |
|---|---|---|
| $^1A_{1g}$ | $^1A$ | $^1A$ |
| $^5T_{2g}$ | $^5A$ | 3A + 2B |
| | $^5A$ | 3A + 2B |
| | $^5B$ | 3B + 2A |
| $^3T_{1g}$ | $^3B$ | B + 2A |
| | $^3A$ | A + 2B |
| | $^3B$ | B + 2A |
| $^3T_{2g}$ | $^3A$ | A + 2B |
| | $^3B$ | B + 2A |
| | $^3A$ | A + 2B |

$S = 2$ throughout the reaction regions (e.g., for $M_3''$ the $^1A_1$ term is lowered by 4 and 21 kcal mol$^{-1}$ at $\Theta = 45$ and 90°, respectively). As suggested (but not required) by the orbital levels in Figure 2, there is no instance of a barrier due to an avoided crossing of the $^1A_1$ surface with another of singlet spin multiplicity along either coordinate. (Such a crossing would exist for $M_3''$ but it is so strongly avoided at the orbital level that no hint of a barrier prior to $\Theta = 90°$ is visible.) It is also readily apparent that these surfaces possess too high barriers ($\Delta E_{el} \sim 61$ ($M_3'$) and 69 ($M_3''$) kcal/mol) to account for intramolecular racemization of $Fephen_3^{2+}$. In this regard, the crossings of the $^5A$ and $^1A$ surfaces at $\Phi \sim 14°$ and $\Theta \sim 67°$ are extremely important for a nondissociative mechanism. Intersystem crossing is seen to be necessary for pseudorotation to yield racemization of $Fephen_3^{2+}$. It is satisfying that $\Delta E_{el}$ is estimated to be 25 kcal/mol, whereas the experimental value of $E_a$ is 29 kcal/mol.[2]

In comparing $M_3'$ and $M_3''$ with regard to the thermal activations to reach the surface intersections, there is little influence from the metal-ligand bonding over the preferred pathway. Selection of the $M_3'$ or $M_3''$ reaction channel is easily dominated by factors not included in the present calculation: interligand interactions, cation association with solvent or anions, and solvent cage rigidity. As an aside, such factors are likely to contribute a few kcal/mol$^{-1}$ to $E_a$ and so diminish an already fortuitously low discrepancy between observed and calculated activation energies (see later).

Noting that $M_3'$ appears as a much "stiffer" mode than $M_3''$ for the lowest singlet and quintet terms, it is perhaps of interest that the stiffer mode is not the less favored for reaching the intersection. Intersystem crossing is achieved at the same energy and halfway along both reaction coordinates.

The shapes of the lowest quintet surfaces take on prime significance for the racemization rates. Both $M_3'$ and $M_3''$ afford facile racemization when the complex has "high-spin" character, unless ligand rigidity for multidentate ligands or steric interactions between bidentate ring systems were to create excessive barriers. In fact, chelates derived from weak ligands with skeletal preference for $D_{3h}$ or $C_{2v}$ geometries appear to be distinctly possible. This characteristic of the quintet surface contrasts sharply with that of the lowest singlet; in fact, low-spin Fe(PccBF) is known[12] to strongly distort toward the antiprism structure, in spite of a marked preference for the prism on the part of PccBF.

**Photoracemization.** An item of interest in photochemical circles is the photoracemization process for ground-state singlet chelates. From our results, the $M_3'$ and $M_3''$ barriers on the lowest singlet excited surfaces are too high for racemization to be competitive with excited-state deactivation. Turning to $^1\Gamma \rightarrow {}^3\Gamma$ intersystem crossing of excited states, even were the internal conversion to proceed with unit efficiency, no significant racemization is expected for the $M_3''$ mode. The best chance for photoracemization arises for slight axial compression along $M_3'$ via the $^1E$, $^3A_2$ intersystem crossing at ~37 $\times 10^3$ cm$^{-1}$. Even were the crossing of high efficiency, a racemization lifetime (based on $\Delta E_{el} > 12$ kcal mol$^{-1}$ on the $^3A_2$ surface) in excess of milliseconds is expected.[13]

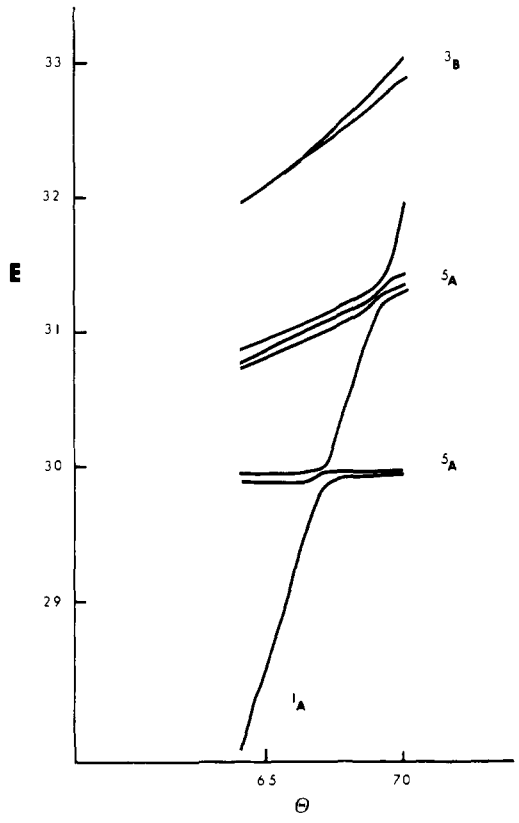


**Figure 4.** The spin-orbit term energies ($\times 10^3$ cm$^{-1}$) for the $M_3''$ mode (A symmetry terms only). Note that the separation of the two lowest $^5A$ levels cannot be resolved on the scale of this figure.

**Intersystem Crossing and Racemization Rates.** Inclusion of $\zeta \sum_i \hat{l}_i \cdot \hat{s}_i$ in the Hamiltonian permits mixing of terms of different $S$ so that many of the crossings in Figure 3 are actually avoided by spin-orbit mixing. Spin selection rules prevent first-order mixing of singlet and quintet states, but these crossings become avoided at the level of second order owing to common (first-order) coupling of singlet and quintet terms to triplet terms.

With reference to the $M_3''$ mode,[14] a breakdown from the $O_h$ origins of the terms depicted in Figure 3B is given in Table I. Spin-orbit terms of like symmetry under $C_2'$ are then expected to be resolved into three avoided crossings and two crossings.

Using the term wave functions generated by the CI calculations, the spin-orbit matrix for the lowest 46 spin-orbit terms (corresponding to the four lowest singlet terms, the six lowest triplet terms, and the five quintet terms of Figure 3B) was diagonalized, with the results for $^1A$, the two lowest $^5A$, and the lowest $^3B$ as shown in Figure 4 (only the spin-orbit terms of A symmetry under $C_2'$ are shown). The energy of second-order coupling of the singlet and quintet terms is clearly quite small, being in the range 50–100 cm$^{-1}$. This means that nonadiabatic behavior is characteristic of molecules approaching the crossover region. We will now consider the effect of this behavior by comparing the observed frequency of racemization of $Fephen_3^{2+}$ with that predicted by the curves of Figures 3 and 4 and the Laudau–Zener approximation[15] for treating reactions with appreciable nonadiabatic character. First we will discuss the theoretical predictions and then compare with experiment.

Lohr has recently reported[16] an analysis of the singlet–triplet intersystem crossing along pseudorotational reaction coordinates for the $T_d \rightleftarrows D_{4h}$ equilibrium of $d^8$ complexes. A

thumbnail review of his analysis is given here for completeness' sake. The Landau–Zener probability for nonadiabatic behavior at a surface crossing (the $^1A$–$^5A$ crossing for the $M_3''$ mode, for example) is written

$$P_{nad} = \exp\left[\frac{-2\pi}{\hbar v|\Delta s|}\epsilon^2\right]$$

where $|\Delta s|$ is the magnitude of the difference in slopes of the intersecting surfaces at the point of intersection. $v$ is the magnitude of the velocity of the moving atom or submolecular fragment at the crossing and is given by

$$v = \left[\frac{2(E - V_c)}{m}\right]^{1/2}$$

In this last expression $E$ is the total energy in the reaction coordinate of a molecule traversing the intersection, $V_c$ is the potential energy at the crossing, and $m$ is the reduced mass of the moving fragments. Finally, in the expression for $P_{nad}$, the quantity $\epsilon$ represents the energy displacements of the actual surfaces from their common energy at the intended crossing.

Lohr has shown that there is advantage to writing $P_{nad}$ in the form

$$P_{nad} = \exp(-x/y^{1/2})$$

$$\text{where } x \equiv (2m)^{1/2}\pi\epsilon^2/\hbar|\Delta s|(kT)^{1/2}$$

$$\text{and } y \equiv (E - V_c)/kT$$

$kT$ is introduced to allow Boltzmann averaging of the total coordinate energy $E$. Specifically, the adiabatic probability is written

$$P_{ad} = 1 - P_{nad} = 1 - \exp(-x/y^{1/2})$$

If the surface crossing is followed by a surface maximum, an additional probability factor, $P_{Ar}$, must be introduced for the net reaction probability:

$$P_r = P_{ad}P_{Ar}$$

Averaging of $P_r$ over all $E$ at temperature $T$ leads to (see Appendix)

$$\bar{P}_r = \exp(-E^{\ddagger}/RT)[1 - \phi_0(\Delta E,x)/\exp(-\Delta E/RT)]$$

where

$$\Delta E = E^{\ddagger} - V_c$$

In the event $\Delta E = 0$, as is the case for the $^1A$, $^5A$ crossing of $M_3''$, $\bar{P}_r$ becomes the expression Lohr derived:

$$\bar{P}_r = \exp(-V_c/RT)[1 - \phi_0(x)]$$

A connection between these theoretical concepts and an experimental rate constant for intersystem crossing follows from the expression

$$\bar{P}_r\nu = k_r$$

where $\nu$ is the frequency of assaults on the surface intersection and $k_r$ is the reaction rate constant.[17] To obtain $P_r$ we use $V_c = 1.7 \times 10^{-19}$ J mol$^{-1}$ (24 kcal/mol$^{-1}$) and $|\Delta s| = 5.6 \times 10^{-19}$ J mol$^{-1}$ rad$^{-1}$ (both values from Figure 3), $m = 5.8 \times 10^{-44}$ J s$^2$ rad$^{-2}$ for rigid phenanthroline rings synchronously rotating about the $x$ and $y$ axis, and $1 \times 10^{-21}$ J (50 cm$^{-1}$) $\leq \epsilon \leq 2 \times 10^{-21}$ J (100 cm$^{-1}$). This gives $0.3 \leq x \leq 1.1$ and $0.4 \leq [1 - \phi_0(x)] \leq 0.8$ after interpolation of $\phi_0(x)$ from Lohr's plot of $\phi_0(x)$ vs. $x$. $\bar{P}_r$ in the range $5 \times 10^{-19}$ to $1 \times 10^{-18}$ results. Taking $\nu = 10^{12}$ s$^{-1}$ yields $5 \times 10^{-7} < k_r < 10^{-6}$ s$^{-1}$. Note that $[1 - \phi_0(x)]$ is not much less than unity so that the racemization rate is dominated by thermal activation to the singlet–quintet crossing and not much impeded by the efficiency of the adiabatic passage through the spin-flip "bottleneck". In analogy with the $Ni^{2+}$ systems,[16] the spin–orbit effects are sufficiently large in practice to have only a subtle effect on $k$.

The experimental facts[2] regarding the racemization processes are $k_r = 10^{-4}$ s$^{-1}$, $E_a = 29$ kcal/mol, and $\Delta S^{\ddagger} = 21$ eu. From these data, $k_r$ would be $\sim 10^{-8}$ s$^{-1}$ for zero entropy of activation (i.e., from $(ekT/h)\exp(-E_a/RT)$). This suggests that the approximate $e_\sigma$ parameter chosen for the calculations is reasonable. That is, the discrepancy in calculated rate constant translates into only $\sim 0.03$ $\mu$m$^{-1}$ in $e_\sigma$.[18]

The sources of $\Delta S° > 0$ for $S = 0 \rightarrow S = 2$ intersystem crossing in $Fe^{2+}$ complexes have been estimated as follows:[19] $\sim +2$ eu from the change in electronic degeneracy and $\sim 4$ eu from the weakening of the Fe–N bonds, with the remainder to be derived from lowering of the various librational frequencies. Certainly the flatness of the $^5A$ surface relative to that of the $^1A$ surface[20] suggests that the pseudorotation mode should contribute to a positive $\Delta S°$. Unfortunately, no vibrational data are on hand to provide an experimental estimate of this contribution to $\Delta S°$. Given that $\Delta S^{\ddagger}$ for $Fephen_3^{2+}$ racemization in $H_2O$ is $\sim 5$–$10$ eu greater than $\Delta S°$ for typical spin-equilibrium systems,[21] it is reasonable to argue that cation desolvation also makes an important contribution to $\Delta S^{\ddagger}$. Specifically, it is commonly accepted that $H_2O$ inserts into the "major" pockets (along the $C_2$ axes) of $Mphen_3^{n+}$ ions in solution. A recent X-ray structure analysis[22] of $Fephen_3I_2 \cdot 2H_2O$ shows $H_2O$ may insert in the "minor" pockets (along $C_3$) as well. Expulsion of these $H_2O$ molecules, along with general solvent reorganization to accommodate the increase in ion volume at the transition state,[23] should further enhance $\Delta S^{\ddagger}$. Unfortunately, numerical estimates of the desolvation entropies are not available at present.

**Probable Reaction Coordinate.** The preceding analysis is an idealization by which racemization and intersystem crossing are achieved along an angular molecular distortion coordinate only. As implied by Figure 2, progress along the $^1A$ $M_3''$ (or $M_3'$) surface entails greater M–L antibonding from the three occupied MOs and this should be reflected in coupling of a radial coordinate(s) to $M_3''$. The consequence of this is that the calculated activation energy along the pure $M_3''$ path must be somewhat in excess of that of a molecule following a mixed-coordinate least energy path for racemization and intersystem crossing. Testing of this idea by the theoretical methods used here is not possible (the angular overlap model cannot generate a parabolic variation in energy with respect to $r$ because the dependence of $e_\sigma$ on $r$ is unknown). The general level of agreement between the pure pseudorotation theory and experiment for $Fephen_3^{2+}$ suggests that either radial expansion must be moderate along the path to the surface crossing or the theory underestimates the $^1A$, $^5A$ crossing energy along $M_3''$.

To close this section, it should be noted that intersystem crossing in some cases could be achieved without experiencing the full angular distortion for the racemization transition state. This could be important in complexes with severe interligand repulsions, where the crossing is followed by a sizable energy barrier on the $^5A$ surface.

**Spin-Equilibria Phenomena.** The recent literature contains reports of experimental measurements of the kinetic and thermodynamic parameters for ground-state intersystem crossing for a variety of $d^5$, $d^6$, and $d^7$ complexes.[21] Most of the complexes studied would be incapable of *fully* following an $M_3'$ or $M_3''$ coordinate because of ligand rigidity or interligand repulsion; as noted above, however, it may only be necessary for chelates to execute but a small fraction of a pseudorotation to effect surface crossing. This should be particularly true for the very small ($\Delta H° \sim 5$–$10$ kcal/mol) singlet–quintet separation found in these complexes.

In these reports considerable attention has been given to $\kappa$, the so-called transmission coefficient in absolute rate theory, to determine the importance of spin-orbit coupling on $k_r$. The estimated values of $\kappa$ vary considerably; lower limits of $10^{-6}$ and $10^{-2}$ have been cited. The transmission coefficient of the rate-constant studies should correspond to the factor $[1 - \phi_0(\Delta E,x)/\exp(-\Delta E/RT)]$ appearing in the analysis given here. There is no meaningful discrepancy between $\kappa \sim 10^{-2}$ and the value of $\leq 10^{-1}$ encountered here. The discrepancy between $10^{-1}$ and $10^{-6}$ is more serious because it implies that $x \propto m^{1/2}\epsilon^2/|\Delta s|$ is several orders smaller than found here.

Based on our results for rotationally induced intersystem crossing in six-coordinate Fe(II), and on Lohr's results for the rotationally induced crossing in four-coordinate Ni(II), $\kappa$ for pseudorotational modes appears to be somewhat insensitive to the metal, coordination number, and change in spin quantum number. This is because $[1 - \phi_0(x)]$ does not become $\ll 1$ until the Landau-Zener factor $x \ll 1$ ($x_{Fe} \sim 1$ and $x_{Ni} \sim 30$). We feel that the question should be raised whether $\kappa$ for radially induced spin flips should be smaller than for the rotational modes. The key element here is the magnitude of $m^{1/2}\epsilon^2/|\Delta s|$. The reduced masses will be little different for the two modes; it falls to a sharply reduced $\epsilon^2/|\Delta s|$ to produce a small $\kappa$. From the generally greater potential surface curvature for bond stretching than torsional coordinates, $|\Delta s|$ should be considerably greater for the singlet-quintet crossing along a radial distention, particularly in those cases where the quintet surface minimum lies at greater distention than does the crossing. Because of the squared dependence on $\epsilon$, up to a factor of $10^2$ reduction in $x$ from $\epsilon$ might arise for radial activation. While an experimental solution, through synthesis of rotationally or radially contrained chelates, may be possible, theoretical confirmation will have to await reliable methods for estimating the dependence of term energies on Fe-ligand bond distance.

## Conclusions

The primary purpose of these computations was to determine the feasibility of ground-state intersystem crossing along the pseudorotatory racemization paths for low-spin $d^6$ complexes. Surprisingly good agreement with experimental results was obtained for the estimates of the parameters used in the calculation. Furthermore, $\kappa$ is not appreciably lowered by the second-order spin-flip bottleneck at the singlet-quintet crossing in the case of pseudorotational activation. It appears possible that $\kappa$ is smaller for radial activation. While the calculational method used here cannot directly test the possibility that term crossing is achieved for $Fephen_3^{2+}$ along a reaction coordinate primarily bond stretching in character, with a subsequently facile racemization via $M_3'$ or $M_3''$, they do imply a predominantly pseudorotational reaction coordinate for $Fephen_3^{2+}$ and, more generally, elaborate the mechanism for intersystem crossing. It remains to be seen whether such pseudorotatory modes are generally involved in internal conversion processes or whether their role is incidental. A suitable test would derive from synthesis of chelates which possess ligands capable of radial, but not torsional, flexibility, and vice versa.

**Acknowledgment** is made to the donors of the Petroleum Research Fund, administered by the American Chemical Society, for support of this research. The author wishes to thank K. G. Kay and L. L. Lohr for helpful discussions.

## Appendix. Boltzmann Averaging of $P_r$

In Figure 3 very weak barriers arise along $M_3'$ and $M_3''$ for the lowest quintet surfaces. These barriers could be heightened slightly by interligand repulsions and desolvation effects. Additionally, it might be possible for a molecule to pass nonadiabatically through the lowest singlet-quintet crossing but adiabatically traverse the next lowest crossing, which is followed by a "chemical" barrier. Accordingly, we examined the effect on $\bar{P}_r$ of a chemical barrier subsequent to the intersystem crossing.

With the crossing of surfaces lying below the chemical activation barrier, the probability that a molecule will react is defined by the probability for the coincidence of adiabatic passage through the intersection and passage over the barrier.

$$P_{Ar} = 0 \text{ for } E < E^{\ddagger} \qquad P_{ad} = 0 \text{ for } E < V_c$$

$$P_{Ar} = 1 \text{ for } E \geq E^{\ddagger} \qquad P_{ad} = 1 - \exp(-x/y^{1/2}) \text{ for } E \geq V_c$$

$$P_r = P_{ad}P_{Ar}$$

Boltzmann averaging (not inaccurate when the moments of inertia are large so that the torsional level spacings are small relative to $kT$) arises through

$$\bar{P}_r = \int_0^{\infty} \exp(-E/RT)P_{ad}P_{Ar}\,dE \Big/ \int_0^{\infty} \exp(-E/RT)\,dE$$

From the definition of $y$ it follows that $E = yRT + V_c$, $dE = RT\,dy$, and $E = 0$ implies $y = -V_c/RT$. Substitution into the expression for $\bar{P}_r$ and performing the integrations

$$\bar{P}_r = \exp(-V_c/RT)[\exp(-\Delta E/RT) - \phi_0(\Delta E,x)]$$

$$= \exp(-E^{\ddagger}/RT)[1 - \phi_0(\Delta E,x)/\exp(-\Delta E/RT)]$$

where

$$\Delta E = E^{\ddagger} - V_c$$

and

$$\phi_0(\Delta E,x) = \int_{\Delta E/RT}^{\infty} \exp(-y)\exp(-x/y^{1/2})\,dy$$

By numerical integration methods we find that the function in brackets only ranges from 0.7 to 0.5 for the representative values of $x = 1$ and $0.6 \leq \Delta E \leq 12.6$ kcal/mol$^{-1}$. This is an interesting result, parallel to that given in the text, since it suggests that the racemization rate is not very sensitive to the surface crossing bottleneck in cases where $x$ is not $\ll 1$ and a chemical activation barrier is preceded by a "spin-forbidden" crossing. Consequently, racemization via the second lowest $^5A$ surface in Figure 3B is negligible relative to the lowest $^5A$ surface because of the additional $4 \times 10^3$ cm$^{-1}$ of thermal activation required. Additionally, the imposition of a several kcal mol$^{-1}$ steric barrier upon the lowest $^5A$ surface will only affect the rate constant significantly by the thermal activation barrier increase ($E^{\ddagger} > V_c$).

## References and Notes

(1) K. F. Purcell and J. P. Zapata, *Chem. Commun.*, 497 (1970).
(2) (a) F. Basolo and R. G. Pearson, "Mechanisms of Inorganic Reactions", 2nd ed., Wiley, New York, 1967, p 314; (b) G. A. Lawrence and D. R. Stranks, *Inorg. Chem.*, **17**, 1804 (1978).
(3) N. R. Davies, *Rev. Pure Appl. Chem.*, **4**, 66 (1954).
(4) C. E. Schäffer and C. K. Jorgensen, *Mol. Phys.*, **9**, 401 (1965); C. E. Schaffer, *Struct. Bonding (Berlin)*, **5**, 68 (1968).
(5) J. K. Burdett, *Inorg. Chem.*, **16**, 3013 (1977); J. Glerup, O. Monsted, and C. E. Schäffer, *Ibid.*, **15**, 1399 (1976).
(6) E. König and R. Schnäkig, *Inorg. Chim. Acta*, **7**, 383 (1973).
(7) J. I. Musher, *Inorg. Chem.*, **11**, 2335 (1972).
(8) C. S. Springer, Jr., and R. E. Sievers, *Inorg. Chem.*, **6**, 852 (1967).
(9) P. Rây and N. K. Dutt, *J. Indian Chem. Soc.*, **20**, 81 (1943).
(10) R. G. Pearson, "Symmetry Rules for Chemical Reactions", Wiley, New York, 1976, p 16.
(11) Eigensystem Subroutine Package, J. M. Boyle et al., "NATS: a Collaborative Effort to Certify and Disseminate Mathematical Software", National ACM Conference, Aug 1972; Anonymous, "The Certified Eigensystem Package, EISPACK", *SIGNUM Newsl.*, **7**, 4 (1972).
(12) M. R. Churchill and A. H. Reis, Jr., *Inorg. Chem.*, **11**, 2299 (1972); E. Larsen, G. N. LaMor, B. E. Wagner, J. E. Parks, and R. H. Holm, *ibid.*, **11**, 2652 (1972).
(13) Surprisingly little information is available on this topic. The most recent monograph on transition-metal photochemistry (A. W. Adamson and P. D. Fleischauer, Eds., "Concepts of Inorganic Photochemistry", Wiley, New

York, 1975) mentions only $Cr^{3+}$ photoracemization. Reference 2a notes that photoracemization accompanies photoredox processes for $Co^{3+}$ and $Rh^{3+}$ oxalato complexes.
(14) One reason that we emphasize only the $M_3''$ mode in this analysis is that, with the high expense of such calculations, a full analysis of the $M_3'$ mode is difficult to justify when there is little difference in the surfaces at the CI level; another reason is that the $M_3''$ mode is favored for phenanthroline by smaller interligand repulsions from the 2,9 protons. That the lowest triplet term lies closer to the $^1A/^5A$ intersection for the $M_3''$ mode than for $M_3'$ turns out to be of little significance: comparison of CI + LS calculations for both modes 1° prior to the crossing shows comparable mixing of $^1A$ and $^5A$ terms.
(15) P. Zener, *Proc. R. Soc. London, Ser. A*, **137**, 696 (1933); **140**, 660 (1933); L. Landau, *Phys. Z. Sowjetunion*, **2**, 46 (1932); H. Eyring, J. Walter, and G. E. Kimball, "Quantum Chemistry", Wiley, New York, 1944, pp 326–330.
(16) L. L. Lohr, Jr., and E. K. Grimmelmann, *J. Am. Chem. Soc.*, **100**, 1100 (1978).
(17) More properly one should also thermally average the frequencies of approach; for our purposes this is an unnecessary elaboration of the theory. The idea here is only to see if a typical bending mode frequency is compatible with the experimental rate constant. Alternately, one could compute the number of crossings required for half-reaction and divide by the experimental half-life to obtain a frequency of assaults on the surface crossing; this should be compatible with $\nu \sim 10^{12}$ s$^{-1}$ (see ref 16). Also, since we are interested in the racemization rate constant we should allow for the fact that two singlet–quintet crossings are required. The probability for this is $2P_t(1 - P_t) = 2P_t$ when $P_t$ is $\ll 1$.
(18) Interestingly, this discrepancy is also on the same order as the $\pi$ bonding parameter, $e_\pi$, which appears appropriate for phen with first row metals; $e_\pi$ has been ignored in these calculations.
(19) M. Sorai and S. Seiki, *J. Phys. Chem. Solids*, **35**, 555 (1974).
(20) The flatness of the $^5A$ surface is probably not unique to the $M_3''$ surface in the sense that the $^5A$ surface is probably flatter than $^1A$ along several metal–ligand coordinates. Note, however, that the flatness of $^5A$ in Figure 3 arises in the absence of interligand repulsion.
(21) E. V. Dose, M. A. Hoselton, N. Sutin, M. F. Tweedle, and L. J. Wilson, *J. Am. Chem. Soc.*, **100**, 1141 (1978); J. P. Jesson, S. Trofimenko, and D. R. Eaton, *ibid.*, **89**, 3158 (1967); J. K. Beattie, R. A. Binstead, and R. J. West, *ibid.*, **100**, 3044 (1978); K. F. Purcell, J. S. Eck, and R. M. Meury, *Inorg. Chem.*, submitted.
(22) L. Hohansson, M. Molund, and A. Oskarsson, *Inorg. Chim. Acta*, **31**, 117 (1978).
(23) G. A. Lawrance and D. R. Stranks, *Inorg. Chem.*, **17**, 1804 (1978).

# Time Development of Nuclear Overhauser Effects in Multispin Systems

**Aksel A. Bothner-By* and J. H. Noggle**

*Contribution from the Department of Chemistry, Carnegie-Mellon University, Pittsburgh, Pennsylvania 15213, and the Department of Chemistry, University of Delaware, Newark, Delaware 19711.* *Received January 25, 1979*

**Abstract:** Two methods are presented for the computation of the time development of $z$ magnetizations in multispin systems during and following application of irradiation at the resonance frequency of one of the spins. Method A includes explicit consideration of the response of the irradiated nucleus to the irradiating field, and can be used in cases where the irradiating power is low ($\gamma H_2 \lesssim 1/T_1$). Method B assumes instantaneous saturation, and is appropriate when high irradiating power is used. In both cases the spin systems are assumed to consist of nuclei with distinct chemical shifts and negligible coupling constants. Sample calculations were performed on model proton systems, assuming long correlation times, typical of larger proteins or other biomacromolecules. These demonstrate that the time dependence of the nuclear Overhauser effect can be used in such systems to investigate relative internuclear distances and to probe for gaps separating islands or chains of nuclei. The use of high irradiating power is shown to be desirable.

## Introduction

Steady-state NOEs have been much exploited for the establishment of spatial proximity between pairs of nuclei in complex molecules.[2] However, when the molecular weight becomes large enough that $\omega\tau_c \gg 1$ (for example, for all but the smallest proteins), the occurrence of spin diffusion causes the steady-state NOEs to be quite nonselective. For intermediate weight proteins, the existence of gaps separating groups of protons in the system will restore some selectivity, but little information can be obtained on spatial arrangement within the groups.[6]

In order to overcome this difficulty, one may observe the changes in intensity at short times after initiating irradiation. The macroscopic magnetization of the irradiated nuclei is then reduced more or less quickly to zero. Those nearby nuclei which cross-relax strongly with the irradiated nucleus will be excited quickly, and will be expected to show a NOE at short times. As spin diffusion occurs, nuclei more remote will also show effects. Thus the time dependence can be used to establish spatial proximity, restoring the capability lost by spin diffusion.

Wüthrich et al.[7,8] have demonstrated the value of this approach, applying it to the assignment of proton signals in the spectra of bovine pancreatic trypsin inhibitor and of horse heart ferricytochrome *c*.

The detailed calculation of the time dependences of the NOEs in a multispin system after initiation of irradiation at time $t = 0$ may be performed in several ways. We present two methods here applicable to polyspin systems where $\delta > J$ for all interacting spins; in the first, an explicit calculation of the effect of the irradiating field on the irradiated nucleus is included, so that cases where $\gamma H_2$ is comparable to or less than the cross-relaxation rate may be analyzed. The second method is applicable to the situation where a strong irradiating field is used so that saturation is, in effect, instantaneous. A simpler analysis is then possible. In the limit of strong irradiating fields the two methods lead to identical results.

## Methods of Calculation

**Method A.** In this case the approach starts with the density matrix equations,[9] using the normal (or magnetization) mode coordinates of Werbelow and Grant,[10] giving

$$d\nu_i/dt + \sum_j \Gamma_{ij}\nu_j = -\omega_2 V_i \qquad (1)$$

Here $\nu_i = M_z^i - M_0^i$ is the $z$ magnetization of one of the spins, and $V_i$ is the sum over all of the transitions of spin $i$ of the "$V$-mode" elements $v_{kl}$. In this paper we ignore the normal mode elements which do not correspond to $z$ magnetiza-

* Carnegie-Mellon University.

0002-7863/79/1501-5152$01.00/0 